
A Space Mapping Approach for the p -Laplace Equation

Oliver Lass¹ and Stefan Volkwein²

¹ Fachbereich Mathematik und Statistik, Universität Konstanz, Universitätsstraße 10, D-78457 Konstanz, Germany. oliver.lass@uni-konstanz.de

² Fachbereich Mathematik und Statistik, Universität Konstanz, Universitätsstraße 10, D-78457 Konstanz, Germany. stefan.volkwein@uni-konstanz.de

Summary. Motivated by car safety applications the goal is to determine a thickness coefficient in the nonlinear p -Laplace equation. The associated optimal problem is hard to solve numerically. Therefore, the computationally expensive, nonlinear p -Laplace equation is replaced by a simpler, linear model. The space mapping technique is utilized to link the linear and nonlinear equations and drives the optimization iteration of the time intensive nonlinear equation using the fast linear equation. For this reason an efficient realization of the space mapping is utilized. Numerical examples are presented to illustrate the advantage of the proposed approach.

1 Introduction

A main aspect in the design of passenger cars with respect to pedestrian safety is the energy absorption capability of the car parts. Besides that, the car parts have to fulfill several other requirements. The associated optimal problem is hard to solve numerically. That makes it necessary to develop easy and fast to solve prediction models with little loss in accuracy for optimization purpose. Current simulation tools combined with standard optimization software are not well suited to deal with the above mentioned needs [13].

We will show the application of mathematical methods on a simplified model to reduce the optimization effort. The goal of the structural optimization problem (see [7, 8]) is to determine a thickness parameter λ of a plate $\Omega \subset \mathbb{R}^2$ (representing a part of the vehicle) and an associated displacement u satisfying the nonlinear p -Laplace equation

$$-\operatorname{div} \left(2(1+n)\lambda(\mathbf{x}) |\nabla u(\mathbf{x})|_2^{2n} \nabla u(\mathbf{x}) \right) = g(\mathbf{x}) \quad \text{for all } \mathbf{x} \in \Omega \quad (1)$$

together with Dirichlet boundary conditions, where g represents a force acting on Ω , $n \in (0, 1)$ is the Hollomon coefficient, and $|\cdot|_2$ stands for the Euclidean norm. We suppose that $0 < \lambda_a \leq \lambda(\mathbf{x}) \leq \lambda_b$ with positive scalars λ_a and λ_b . Our goal is to minimize the mass of the plate, i.e., to minimize the integral

$$J_1(\lambda) = \int_{\Omega} \lambda(\mathbf{x}) \, d\mathbf{x}$$

but also to avoid that the displacement is larger than a given threshold $u_b > 0$. This issue is motivated by our pedestrian safety application. Thus we choose

$$J_2(u) = \beta \int_{\Omega} \min(u(\mathbf{x}) - u_b(\mathbf{x}), 0)^3 \, d\mathbf{x}$$

as the second part of our cost functional. Here $\beta > 0$ is a weighting parameter. Due to the nonlinear structure of the elliptic partial differential equation, the numerical solution of the optimization problem governed by the partial differential equation (PDE) constraint (1) is expensive, we consider an alternative constraint given by

$$-\operatorname{div}(2(1+n)\mu(\mathbf{x})\nabla v(\mathbf{x})) = g(\mathbf{x}) \quad \text{for all } \mathbf{x} \in \Omega, \quad (2)$$

which is a linear elliptic PDE. We will call (1) the fine model and (2) the coarse model. It turns out that the space mapping technique [9] provides an attractive framework to improve the use of the coarse model as a surrogate for the optimization of the fine model. The space mapping technique is utilized to link the linear and nonlinear equations and drives the optimization iteration of the time intensive nonlinear equation using the fast linear equation. For this reason an efficient realization of the space mapping is utilized.

The space mapping technique was first introduced in [2]. The idea of the space mapping has been developed along different directions and generalized to a number of contexts [14]. One of the problems lies in the information necessary to compute the Jacobian of the space mapping which involves expensive gradient information of (1). In [1] Broyden's method is utilized to construct an approximation of the Jacobian. This approach will be presented. In the context of PDEs, we refer to [6, 10]. Compared to [1, 2, 14], our modified approach is similar to [6], where a modified Broyden formula is used.

The paper is organized in the following manner. In Section 2 we introduce the infinite-dimensional optimization problem for the p -Laplace equation. The space mapping approach is described in Section 3, whereas in Section 4 the surrogate optimization problem is formulated. Section 5 is devoted to present numerical examples illustrating the advantage of the proposed approach.

2 Optimization of the complex model

In this section we formulate optimal control problem governed by the p -Laplace equation. By $W_0^{1,p}(\Omega)$, $p \in [1, \infty)$, we denote the Sobolev space of weakly differentiable functions, whose weak derivative belongs to $L^p(\Omega)$ and whose function values are zero on the boundary $\Gamma = \partial\Omega$. We set $p = 2n + 2$ for $n \in (0, 1)$. Let us define the Banach space $X = L^\infty(\Omega) \times W_0^{1,p}$ and the nonlinear operator $f : X \rightarrow W_0^{1,p}(\Omega)'$ (*fine model*) as

$$\langle f(x), \varphi \rangle_{(W_0^{1,p})', W_0^{1,p}} = \int_{\Omega} 2(1+n)\lambda(\mathbf{x})|\nabla u(\mathbf{x})|_2^{p-2}\nabla u(\mathbf{x})\cdot\nabla\varphi(\mathbf{x})-g(\mathbf{x})\varphi(\mathbf{x})\,dx$$

for $x = (\lambda, u) \in X$ and $\varphi \in W_0^{1,p}(\Omega)$, where $\langle \cdot, \cdot \rangle_{(W_0^{1,p})', W_0^{1,p}}$ denotes the dual pairing between $(W_0^{1,p}(\Omega))'$ and $W_0^{1,p}(\Omega)$. Now $f(x) = 0$ in $(W_0^{1,p}(\Omega))'$ for $x = (\lambda, u) \in X$ is equivalent with the fact that u is a weak solution to (1) for thickness parameter λ .

The goal is to determine an optimal thickness parameter λ and a corresponding optimal displacement u minimizing the cost functional $J_f : X \rightarrow \mathbb{R}$ given by

$$J_f(x) = \int_{\Omega} \lambda(\mathbf{x}) + \frac{\eta}{2} |\lambda(\mathbf{x}) - \lambda^\circ(\mathbf{x})|^2 + \beta \min(u(\mathbf{x}) - u_b(\mathbf{x}), 0)^3 \, dx$$

for $x = (\lambda, u) \in X$ subject to (s.t.) the equality constraints $f(x) = 0$ in $(W_0^{1,p}(\Omega))'$ and to the inequality constraints $\lambda_a \leq \lambda(\mathbf{x}) \leq \lambda_b$ f.a.a. $\mathbf{x} \in \Omega$, where λ_a, λ_b are positive scalars with $\lambda_a \leq \lambda_b$, $\eta \geq 0$ is a regularization parameter and $\lambda^\circ \in C^{0,1}(\overline{\Omega})$ is a nominal thickness parameter satisfying $\lambda_a \leq \lambda^\circ(\mathbf{x}) \leq \lambda_b$ f.a.a. $\mathbf{x} \in \Omega$. Furthermore, $\beta \geq 0$ is a weighting parameter and $u_b \in L^\infty(\Omega)$ satisfies $u_b(\mathbf{x}) > 0$ f.a.a. $\mathbf{x} \in \Omega$. The last term of the cost functional J_f penalizes the situation if the displacement is larger than the given threshold u_b . We introduce the set of admissible thickness parameters by

$$A_{ad} = \{ \lambda \in C^{0,1}(\overline{\Omega}) \mid \lambda_a \leq \lambda(\mathbf{x}) \leq \lambda_b \text{ f.a.a. } \mathbf{x} \in \Omega \text{ and } \|\lambda\|_{C^{0,1}(\overline{\Omega})} \leq c_b \}$$

with $c_b = \|\lambda_b\|_{C^{0,1}(\overline{\Omega})}$ and define $X_{ad} = A_{ad} \times W_0^{1,p}(\Omega)$. Then, the infinite-dimensional, nonconvex minimization problem can be formulated abstractly as

$$\min J_f(x) \quad \text{s.t.} \quad x \in \mathcal{F}_f = \{ x \in X_{ad} \mid f(x) = 0 \text{ in } (W_0^{1,p}(\Omega))' \}, \quad (3)$$

where \mathcal{F}_f is the set of admissible solutions. Let us refer to [4, 5] for optimal solutions existence results for (3), where a Dirichlet and Neumann optimal control problem governed by the p -Laplace equation is considered.

Solving (1) numerically is a difficult task due to the quasilinear elliptic constraint $f(x) = 0$ (fine model). In the next section we utilize instead of the accurate, but complex model (1) a linear elliptic PDE as a simpler model that is much easier to solve. Then we combine the simple and the complex model by applying a space mapping approach.

3 Space mapping

The space mapping is a mapping between the fine model space parameter or variables and the coarse model space. Then the optimization can be carried out for the coarse model, but information from the fine model is utilized to improve the accuracy of the optimization result with respect to the real application.

As introduced in Section 1 the goal is to replace the fine model (1) by the coarse model (2). Later this fine model will be used in the optimization problem. Existence and uniqueness of a weak solution to (2) were discussed in [3]. Let us now define the Banach space $Y = L^\infty(\Omega) \times H_0^1(\Omega)$ and introduce the bilinear operator $c : Y \rightarrow H^{-1}(\Omega)$ (*coarse model*) by

$$\langle c(y), \varphi \rangle_{H^{-1}, H_0^1} = \int_{\Omega} 2(1+n)\mu(\mathbf{x})\nabla v(\mathbf{x}) \, d\mathbf{x} - \langle g, \varphi \rangle_{H^{-1}, H_0^1}$$

for $y = (\mu, v) \in Y$ and $\varphi \in H_0^1(\Omega)$, where $\langle \cdot, \cdot \rangle_{H^{-1}, H_0^1}$ stands for the dual pairing between $H_0^1(\Omega)$ and its dual space $H^{-1}(\Omega)$.

Let us now formulate the space mapping. Our fine model is the p -Laplace equation (1) with the model output u together with the thickness parameter λ . The coarse model is given by the linear elliptic PDE (2) with the model output v and the thickness parameter μ . The goal of the space mapping is to adjust the thickness parameter μ in the coarse model so that the model outputs u and v are similar. Furthermore we want to achieve that the thickness parameters μ and λ are not too distinct.

Concentrating on the region of interest (the subset of Ω , where the force g acts) we consider the space mapping on a subset $\mathcal{A} \subseteq \Omega$. We define the restriction operator $\mathcal{R}_{\mathcal{A}} : L^2(\Omega) \rightarrow L^2(\Omega)$ as $\mathcal{R}_{\mathcal{A}}v = v$ on \mathcal{A} a.e. and $\mathcal{R}_{\mathcal{A}}v = 0$ otherwise. Further we introduce the set of admissible thickness parameters by

$$M_{ad} = \left\{ \mu \in C^{0,1}(\overline{\Omega}) \mid \mu_a \leq \mu(\mathbf{x}) \leq \mu_b \text{ f.a.a. } \mathbf{x} \in \Omega \text{ and } \|\mu\|_{C^{0,1}(\overline{\Omega})} \leq C_b \right\}$$

with $C_b = \|\mu_b\|_{C^{0,1}(\overline{\Omega})}$. For $\mu \in M_{ad}$ the solution to (2) belongs to $H^2(\Omega)$.

Now we introduce the *space mapping* $\mathcal{P} : \Lambda_{ad} \rightarrow M_{ad}$ as follows: for a given thickness parameter $\lambda \in \Lambda_{ad}$ the corresponding $\mu = \mathcal{P}(\lambda) \in M_{ad}$ is the thickness parameter so that $\mathcal{R}_{\mathcal{A}}v$ is as close as possible to $\mathcal{R}_{\mathcal{A}}u$. We formulate μ as the solution to a minimization problem. The goal is to determine an optimal thickness μ for a given λ minimizing the cost functional $J_{sp} : Y \rightarrow \mathbb{R}$ given by

$$J_{sp}(y) = \frac{\gamma}{2} \int_{\mathcal{A}} |v(\mathbf{x}) - u(\mathbf{x})|^2 \, d\mathbf{x} + \frac{\kappa}{2} \int_{\Omega} |\mu(\mathbf{x}) - \lambda(\mathbf{x})|^2 \, d\mathbf{x}$$

for $y = (\mu, v) \in Y$ subject to $\mu \in M_{ad}$ and the equality constraint $c(y) = 0$ in $H^{-1}(\Omega)$, where $\gamma > 0$ is a weighting and $\kappa \geq 0$ is a smoothing parameter.

Let us now formulate the minimization problem more abstractly. We define $Y_{ad} = M_{ad} \times H_0^1(\Omega)$, then the problem can then be written as follows

$$\min J_{sp}(y) \quad \text{s.t.} \quad y \in \mathcal{F}_{sp} = \{y \in Y_{ad} \mid c(y) = 0 \text{ in } H^{-1}(\Omega)\}, \quad (\mathbf{P}_{sp})$$

where \mathcal{F}_{sp} is the set of admissible solutions.

The following theorem ensures existence of optimal solutions to (\mathbf{P}_{sp}) and states the first-order necessary optimality conditions. The proof follows from [3] and [8].

Theorem 1. *The problem (\mathbf{P}_{sp}) has at least one optimal solution $y^* = (\mu^*, v^*) \in Y_{ad}$, which can be characterized by first-order necessary optimality conditions: There exists a unique associated Lagrange multiplier $p^* \in V$ together with y^* satisfying the adjoint equation*

$$\begin{aligned} -\operatorname{div} (2(1+n)\mu^*(\mathbf{x})\nabla p^*(\mathbf{x})) &= -\gamma(\mathcal{R}_{\mathcal{A}}(v^* - u))(\mathbf{x}) && \text{f.a.a. } \mathbf{x} \in \Omega, \\ p^*(\mathbf{x}) &= 0 && \text{f.a.a. } \mathbf{x} \in \Gamma. \end{aligned} \quad (4)$$

Moreover, the variational inequality

$$\int_{\Omega} (\kappa(\mu^*(\mathbf{x}) - \lambda(\mathbf{x})) + 2(1+n)(\nabla v^*(\mathbf{x}) \cdot \nabla p^*(\mathbf{x}))) (\mu_{\delta}(\mathbf{x}) - \mu^*(\mathbf{x})) \, d\mathbf{x} \geq 0$$

holds for all $\mu_{\delta} \in M_{ad}$.

The optimal control problem given by (\mathbf{P}_{sp}) can be written in reduced form

$$\min \hat{J}_{sp}(\mu) \quad \text{s.t. } \mu \in M_{ad}. \quad (\hat{\mathbf{P}}_{sp})$$

The gradient of the reduced cost functional at a given point $\mu \in M_{ad}$ in a direction $\mu_{\delta} \in L^{\infty}(\Omega)$ is given by

$$\hat{J}'_{sp}(\mu)\mu_{\delta} = \int_{\Omega} (\kappa(\mu(\mathbf{x}) - \lambda(\mathbf{x})) + 2(1+n)\nabla v(\mathbf{x}) \cdot \nabla p(\mathbf{x})) \mu_{\delta}(\mathbf{x}) \, d\mathbf{x},$$

where v satisfies (2) and p solves (4).

In our numerical experiments we assume that $(\hat{\mathbf{P}}_{sp})$ has an inactive solution μ^* , i.e., $\mu_a < \mu^* < \mu_b$ f.a.a. $\mathbf{x} \in \Omega$ and $\|\mu^*\|_{C^{0,1}(\Omega)} < C_b$. We utilize a globalized Newton method with Armijo backtracking line search algorithm [12, p. 37] to solve $(\hat{\mathbf{P}}_{sp})$. In each level of the Newton method the linear system

$$\hat{J}''_{sp}(\mu^{\ell})d^{\ell} = -\hat{J}'_{sp}(\mu^{\ell}) \quad (5)$$

is solved by the truncated conjugate gradient method [12, p. 169]. We find

$$(\hat{J}''_{sp}(\mu^{\ell})\mu_{\delta})(\mathbf{x}) = \kappa\mu_{\delta}(\mathbf{x}) + 2(1+n)(\nabla v_{\delta}(\mathbf{x}) \cdot \nabla p^{\ell}(\mathbf{x}) + \nabla v^{\ell}(\mathbf{x}) \cdot \nabla p_{\delta}(\mathbf{x}))$$

f.a.a. $\mathbf{x} \in \Omega$, where u^{ℓ} and p^{ℓ} satisfy (2) and (4) respectively and u_{δ} and p_{δ} satisfy linearized state and adjoint equations; see [8]. Another possibility to solve (5) is to utilize a quasi Newton approximation or the Hessian.

4 Surrogate optimization

In this subsection we turn to the surrogate optimization that is used to solve approximately (3). The main idea is to solve the optimization problem using the coarse model $c(y) = 0$, but to take the fine model $f(x) = 0$ into account by the space mapping technique introduced in Section 3.

Let us introduce the Banach space $Z = L^\infty(\Omega) \times H_0^1(\Omega)$ and the subset $Z_{ad} = \Lambda_{ad} \times H_0^1(\Omega)$. We define the cost functional $J_{so} : Z \rightarrow \mathbb{R}$ as

$$J_{so}(z) = \int_{\Omega} \lambda(\mathbf{x}) + \frac{\eta}{2} |\lambda - \lambda^\circ|^2 + \beta \min(v(\mathbf{x}) - u_b(\mathbf{x}), 0)^3 \, d\mathbf{x}$$

for $z = (\lambda, v) \in Z$, where $\eta, \lambda^\circ, \beta, u_b$ are as in Section 2. We consider the optimization problem

$$\min J_{so}(z) \quad \text{s.t.} \quad z \in \mathcal{F}_{so} = \{z \in Z_{ad} \mid c(\mu, v) = 0 \text{ and } \mu = \mathcal{P}(\lambda)\}. \quad (\mathbf{P}_{so})$$

Note that in the surrogate optimization the space mapping is used to link the coarse and the fine model and therefore informations of the fine model are taken into account in the optimization process. We suppose that (\mathbf{P}_{so}) has a local optimal solution $z^* = (\lambda^*, v^*) \in Z_{ad}$. In particular, we have $v^* = \mathcal{S}_c(\mathcal{P}(\lambda^*))$, where \mathcal{S}_c denotes the solution operator for the coarse model. The corresponding reduced problem is given by

$$\min \hat{J}_{so}(\lambda) \quad \text{s.t.} \quad \lambda \in \Lambda_{ad}$$

with

$$\hat{J}_{so}(\lambda) = \int_{\Omega} \lambda(\mathbf{x}) + \frac{\eta}{2} |\lambda - \lambda^\circ|^2 + \beta \min(v(\mathbf{x}) - u_b(\mathbf{x}), 0)^3 \, d\mathbf{x}, \quad \lambda \in \Lambda_{ad}$$

with $v = \mathcal{S}_c(\mathcal{P}(\lambda))$. Next we state the first-order necessary optimality conditions for (\mathbf{P}_{so}) ; see [7].

Theorem 2. *Suppose that $z^* = (\lambda^*, v^*)$ is a local solution to (\mathbf{P}_{so}) and the space mapping \mathcal{P} is Fréchet-differentiable. Then there exist unique associated Lagrange multipliers $p^* \in V$ and $\xi^* \in L^2(\Omega)$ together with z^* satisfying the adjoint equation*

$$\begin{aligned} -\operatorname{div}(2(1+n)\mu^*(\mathbf{x})\nabla p^*(\mathbf{x})) &= -3\beta \min(v^*(\mathbf{x}) - u_b(\mathbf{x}), 0)^2 \quad \text{f.a.a. } \mathbf{x} \in \Omega, \\ p^*(\mathbf{x}) &= 0 \quad \text{f.a.a. } \mathbf{x} \in \Gamma. \end{aligned}$$

Moreover, the variational inequality

$$\int_{\Omega} (1 + \eta(\lambda^*(\mathbf{x}) - \lambda^\circ(\mathbf{x})) + 2(1+n)\mathcal{P}'(\lambda^*)^*(\nabla v^*(\mathbf{x}) \cdot \nabla p^*(\mathbf{x}))) (\lambda_\delta(\mathbf{x}) - \lambda^*(\mathbf{x})) \, d\mathbf{x} \geq 0$$

holds for all $\lambda_\delta \in \Lambda_{ad}$, where $\mathcal{P}'(\lambda^*)^*$ denotes the adjoint operator to $\mathcal{P}'(\lambda^*)$.

It follows that the gradient \hat{J}'_{so} of the reduced cost functional is given by

$$\hat{J}'_{so}(\lambda) = 1 + \eta(\lambda - \lambda^\circ) + \mathcal{P}'(\lambda)^* 2(1+n)\nabla v(\cdot) \cdot \nabla p(\cdot) \quad \text{in } \Omega,$$

where the function v satisfies

$$\begin{aligned} -\operatorname{div} (2(1+n)\mu(\mathbf{x})\nabla v(\mathbf{x})) &= g(\mathbf{x}) \quad \text{f.a.a. } \mathbf{x} \in \Omega, \\ v(\mathbf{x}) &= 0 \quad \text{f.a.a. } \mathbf{x} \in \Gamma \end{aligned}$$

with $\mu = \mathcal{P}(\lambda)$ and p is the solution to

$$\begin{aligned} -\operatorname{div} (2(1+n)\mu(\mathbf{x})\nabla p(\mathbf{x})) &= -3\beta \min(v^*(\mathbf{x}) - u_b(\mathbf{x}), 0)^2 \quad \text{f.a.a. } \mathbf{x} \in \Omega, \\ p(\mathbf{x}) &= 0 \quad \text{f.a.a. } \mathbf{x} \in \Gamma. \end{aligned}$$

To avoid the computation of the operator $\mathcal{P}'(\lambda)$ we apply Broyden's updating formula providing a matrix B which can be used to replace $\mathcal{P}'(\lambda)$, but also $\mathcal{P}'(\lambda)^*$. We use a modified Broyden's update formula introduced in [6]:

$$B_{\ell+1} = B_{\ell} + \frac{\widetilde{\mathcal{P}}_{\delta} - B_{\ell}\lambda_{\delta}}{\|\lambda_{\delta}\|_{L^2(\Omega)}^2} \langle \lambda_{\delta}, \cdot \rangle_{L^2(\Omega)}$$

with

$$\widetilde{\mathcal{P}}_{\delta} = \mathcal{P}_{\delta} + \sigma \frac{\hat{J}_{\delta} - \langle \hat{J}'_{sur}(\lambda^k), \mathcal{P}_{\delta} \rangle_{L^2(\Omega)}}{\|\lambda_{\delta}\|_{L^2(\Omega)}^2} \hat{J}'_{sur}(\lambda^{\ell}),$$

where $\hat{J}_{\delta} = \hat{J}'_{so}(\lambda^{\ell+1}) - \hat{J}'_{so}(\lambda^{\ell})$, $\lambda_{\delta} = \lambda^{\ell+1} - \lambda^k$ and $\mathcal{P}_{\delta} = \mathcal{P}(\lambda^{\ell+1}) - \mathcal{P}(\lambda^{\ell})$. Note that for $\sigma = 0$ we get the classical Broyden's update formula.

For the numerical solution we apply the gradient projection method using Broyden's updating to obtain an approximation of the sensitivity $\mathcal{P}'(\lambda)$.

5 Numerical results

In this section we present numerical results for the space mapping and the surrogate optimization. For our numerical example we consider a domain representing a simplified door, denoted by Ω . The gray line in Figure 2 (left plot) indicates the section of the boundary, where homogeneous Neuman boundary conditions of the form $\langle \nabla u(x), \vec{n} \rangle_2 = 0$ are applied, where \vec{n} denotes an outer normal on the boundary and $\langle \cdot, \cdot \rangle_2$ the Euclidean inner product. We use the finite element discretization and solvers for (1) and (2) provided by the `Matlab Partial Differential Equation Toolbox`. The right-hand side $g(\mathbf{x})$ (force term) is given as follows:

$$g(\mathbf{x}) = \begin{cases} 47.71, & \mathbf{x} \in \mathcal{B}_r(\mathbf{x}_{mid}) = \{\mathbf{x} \in \Omega \mid |\mathbf{x}_{mid} - \mathbf{x}|_2 < r\}, \\ 0, & \text{otherwise,} \end{cases}$$

where $\mathbf{x}_{mid} = (0.5, 0.45)^T$ and $r = 0.1$. This force term is indicated as the gray circle in Figure 2 (left plot). Let us next state the parameters for our numerical example. The Hollomon coefficient is set to $n = 0.22$. For the space mapping we choose the weight parameter as $\gamma = (\int_{\Omega} |u(\mathbf{x})|^2 \, d\mathbf{x})^{-1}$ and $\kappa = 10^{-3}\gamma$. Further we choose the region \mathcal{A} to be a circle with radius 0.2 and midpoint $(0.5, 0.45)$, illustrated in Figure 2 (left plot) by a black circle. Next

we have a look at the parameters for the surrogate optimization. We choose η , β and λ° to be 1.25, 25^5 and 1.7, respectively. The threshold u_b is set to 0.3 and the bounds for the thickness parameter are set to $\mu_a = \lambda_a = 0.05$ and $\mu_b = \lambda_b = 10$. As a stopping criteria we choose the norm of the reduced gradient to be smaller than 0.1 times the maximum diameter of the finite elements. We will report on numerical results for two different settings for the parameter σ .

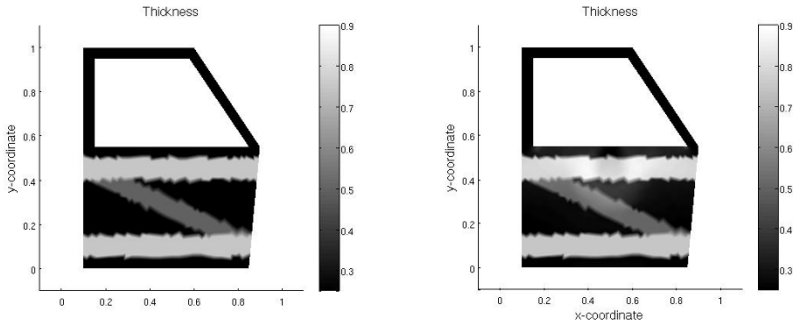


Fig. 1. Initial thickness parameter (left plot) and the optimal thickness parameter μ^* (right plot) for the space mapping using the Newton-CG method.

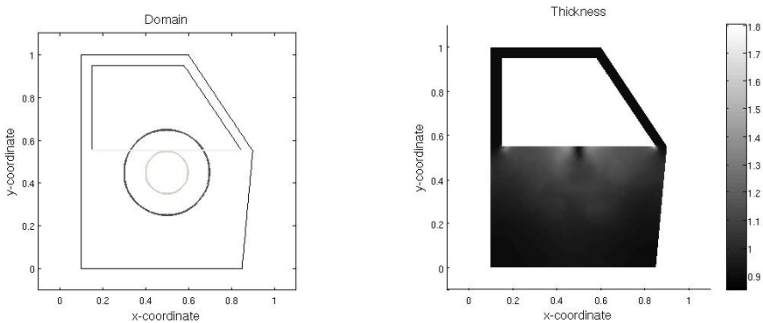


Fig. 2. Domain Ω with region \mathcal{A} (black circle) and region $B_r(\mathbf{x}_{mid})$ (gray circle) (left plot) and the optimal thickness parameter λ^* (right plot) for the surrogate optimization.

Let us first present a numerical result for the space mapping. As an initial thickness for the space mapping we choose a structured initial thickness parameter, shown in Figure 1 (left plot). In the right plot of Figure 1 we present the corresponding thickness parameter μ^* computed by the space mapping. We observe that the thickness parameter is enlarged in the region \mathcal{A} . In Table 1 the numerical results and performance for the space mapping utilizing the

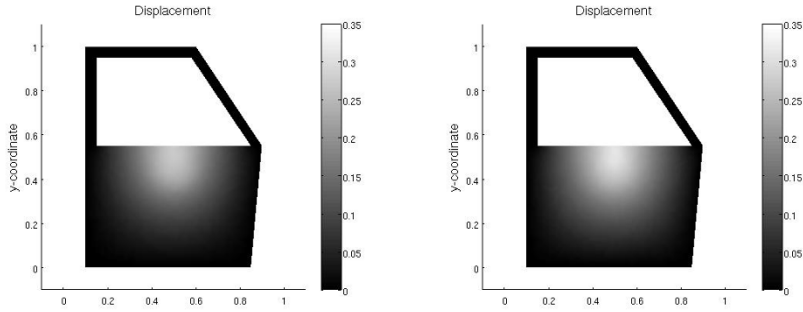


Fig. 3. Displacement v solving (2) for $\mu = \lambda^*$ (left plot) and solution u to (1) for $\lambda = \lambda^*$ (right plot).

Table 1. Summary of the results for the space mapping and the performance for two different methods.

	v	u	BFGS	Newton-CG
\max_{Ω}	0.68961	0.59601	0.59541	0.59462
Iterations			9	4
Time (sec)			8.52	4.81

Table 2. Summary of the results for the surrogate optimization and the performance of the gradient projection method for two different Broyden’s updates ($\sigma = 0$ and $\sigma = 0.2$).

σ	$\max_{\Omega} u$	$\max_{\Omega} v$	Volume	$\min_{\Omega} \lambda$	$\max_{\Omega} \lambda$	$\ u - v\ _{L^2(\Omega)}$	Iter	Time (sec)
0.0	0.31307	0.27650	0.48857	0.89759	1.77613	0.01198	10	82.72
0.2	0.31313	0.27606	0.48899	0.89555	1.67856	0.01204	7	57.65

Newton-CG and the BFGS algorithms are summarized. It turns out that for the thickness parameter shown in Figure 1 (left plot) the maximal displacements for v (solution to the linear model) and u (solution to the p -Laplacian) are quite different. Using the space mapping the optimal thickness parameter leads to a maximal displacement in the linear model that is very close to maximal one of u . Furthermore, we observe from Table 1 that the Newton-CG method performs significantly better than the BFGS method while giving nearly the same results measured in the maximum displacement.

Next we present the numerical results for the surrogate optimization. In Figure 2 (right plot) the optimal thickness parameter λ^* for the surrogate optimization is shown. The corresponding displacements for the coarse and fine model are shown in Figure 3 (left and right plot), respectively. Comparing the plots in Figure 3 we observe that the maximum displacement of the non-linear model is significantly larger than the maximal displacement for the linear model. Therefore, if we make the thickness parameter λ^* smaller, the

maximal displacement for the non-linear model would be significantly larger than the threshold $u_b = 0.3$. The surrogate optimization takes this fact into account. In Table 2 we summarize the numerical results for the two different values for σ . Note that the modified Broyden's update gives a better performance than the classical Broyden's update with respect to the number of iterations and CPU time while giving nearly the same results. Further it is observed that for different initial guesses of λ^0 the algorithm converges to the same numerical solution.

References

1. M.H. Bakr, J.W. Bandler, K. Masden, and J. Søndergaard (2001) An introduction to the space mapping technique. *Optimization and Engineering* 2(4):369–384
2. J.W. Bandler, R.M. Biernacki, Shao Hua Chen, P.A. Grobelny, R.H. Hemmers (1994) Space mapping technique for electromagnetic optimization. *IEEE Transactions on Microwave Theory and Techniques* 42(12):2536–2544
3. E. Casas (1992) Optimal control in coefficients of elliptic equations with state constraints. *Applied Mathematics and Optimization* 26(1):21–37
4. E. Casas, L.A. Fernández (1993) Distributed control of systems governed by a general class of quasilinear elliptic equations. *Journal of Differential Equations* 104(1):20–47
5. E. Casas, L.A. Fernández (1995) Dealing with integral state constraints in boundary control problems or quasilinear elliptic equations. *SIAM Journal on Control and Optimization* 33(2):568–589
6. M. Hintermüller, L.N. Vicente (2005) Space mapping for optimal control of partial differential equations. *SIAM Journal on Optimization* 15(4):1002–1025
7. O. Lass, C. Posch, G. Scharrer, S. Volkwein (Submitted 2009) Space mapping techniques for the optimization of a thickness parameter in the p -Laplace equation.
8. O. Lass (2009) Efficient numerical space mapping techniques for the p -Laplace equation. Diploma thesis, Karl-Franzens-Universität, Graz
9. S.J. Leary, A. Bhaskar, A.J. Keane (2001) A constraint mapping approach to the structural optimization of an expensive model using surrogates. *Optimization and Engineering* 2(4):385–398
10. J. Marburger (2007) Space mapping and optimal shape design. Diploma Thesis, Technische Universität, Kaiserslautern
11. H. Maurer, J. Zowe (1979) First and second order necessary and sufficient optimality conditions for infinite-dimensional programming problems. *Mathematical Programming* 16(1):98–110
12. J. Nocedal, S.J. Wright (2006) *Numerical optimization*, 2. Edition. Springer Series in Operations Research, Springer-Verlag, New York
13. G. Scharrer, S. Volkwein, T. Heubrandtner (2010) Mathematical optimization of the plate volume under a p -laplace partial differential equation constraint by using standard software. To appear in *International Journal of Multiphysics*
14. L.N. Vicente (2003) Space mapping: models, sensitivities, and trust-region methods. *Optimization and Engineering* 4(3):159–175